

2022 S.T. Yau High School Science Award (Asia)

Research Report

The Team

Name of team member: Yunhao Liu

School: The Experimental High School Attached to Beijing Normal University

Country: China

Name of supervising teacher: Mingjie Liu

Job Title: Professor

School: Beihang University

Country: China

Title of Research Report

Large-scale production of nanocomposite membrane with excellent nanofiltration property

Date

10 September 2022

Large-scale production of nanocomposite membrane with excellent nanofiltration property

Yunhao Liu

The Experimental High School Attached to Beijing Normal University, Beijing

100032, China

Abstract:

Sodium alginate (SA), a natural anionic polysaccharide extracted from seaweed, which can be cross-linked by calcium ions, has shown excellent separation performance. However, scale-up of these calcium alginates (CA) filtration membranes to large-area in a universal and viable manner remains an open issue. Here we report a one-step strategy to fabricate CA membranes based on the superspreading of SA solution on immersed hydrogel surfaces. The prepared CA filtration membrane exhibited high retention (> 94%) for positively charged and neutral organic molecules. The results of dye rejection studies demonstrated this nanofiltration membrane has promising application prospects in the fields of protein separation, microorganism filtration and removal of dyes.

Keywords: filtration membrane; calcium alginate; large-scale; superspreading; dyes rejection

Contents

1. Introduction	4
2. Experimental	6
2.1 Materials.....	6
2.2 Preparation of polyacrylamide hydrogel.....	6
2.3 Preparation of calcium alginate filtration membrane.....	7
2.4 Characterization.....	7
3. Results and Discussion	8
3.1 Characterization of calcium alginate filtration membrane.....	8
3.2 Selection of filter dye and determination of standard equation.....	11
3.3 Effect of membrane thickness on filtration performance.....	13
3.4 Filtration property of CA membrane for different dye molecules.....	14
4. Conclusion	17
5. Acknowledgement	18
6. References	19

1. Introduction

Wastewater containing ultrafine nanoparticles causes severe damages to environment and human health, therefore the treatment of ultrafine nanoparticles receives increasing concerns around the world ^[1-4]. Membrane separation technology has become a reliable and promising method for wastewater treatment because of its low cost, high efficiency and easy operation ^[4-6]. However, in the separation process, the inevitable concentration polarization, membrane pollution and clogging of filter holes reduce the operational reliability of membrane filtration equipment, hindering nanofiltration membrane further application in ultrafine nanoparticles treatment. Because of the hydrophobicity of traditional membrane materials, macromolecules, electrolytes or colloidal substances would be irreversible deposited on surface of membrane, leading the severely reduced of membrane flux. Therefore, improving the hydrophilicity of the membrane surface is the effective methods to reduce membrane fouling and improve the filtration efficiency of membrane ^[7]. In the last score years, coating the hydrophilic layer or grafting hydrogel on the surface of membrane have been adopted to avoid the problem of membrane pollution ^[8-11]. Membrane fouling modification can be carried out by blending, surface coating, electrospinning and surface grafting. However, how to fabricate the large-area filtration membrane through low-cost and efficiency method still remains a challenge. Therefore, it is of great importance to propose more advanced and effective strategies to realize the large-area manufacturing of filtration membrane with the excellent performance.

Sodium alginate (SA), a natural macromolecule extracted from Phaeophyta or Sargassum, is an unbranched polysaccharide which is mainly composed of three structural units “mannitol uronic acid-mannitol uronic acid”, “glucuronic acid-glucuronic acid” or “mannitol uronic acid- glucuronic acid” [12]. Owing to the low cost, hydrophilic and excellent biodegradable properties of sodium alginate, extensive efforts have been devoted to investigating the application of sodium alginate [13]. In addition, it has been discovered that sodium alginate can be crosslinked with divalent cations to fabricate ionic hydrogels. Among these divalent cations, calcium ion (Ca^{2+}) has been considered as the best candidate because of excellent biocompatibility [14]. After crosslinked by cations, the SA exhibits the outstanding film-forming ability. That is the reason that SA is widely used to fabricate various films [15-20].

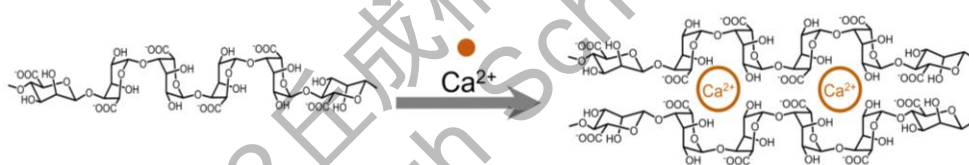


Figure 1. Schematic of Ca^{2+} and sodium alginate polymer crosslinking

The crosslinking mechanism of sodium alginate is mainly the complexation reaction between uronic acid segment and divalent ions. When calcium ion and sodium alginate exist simultaneously, the adjacent polymer chains of SA would be combined with Ca^{2+} to form a complete molecular chain. Subsequently, the adjacent molecular chains are combined through the interaction of hydroxyl groups and hydrogen bonds to construct the network of hydrogel. The structure is similar to the "egg-box" structure, as shown in Figure 1. Therefore, in combination with the characteristics of gel interface

superspreading, calcium alginate (CA) ultra-thin filter membrane is prepared through in-situ polymerization of gel ^[21].

2. Experimental

2.1 Materials

Acrylamide (AAM, J&K Scientific), N,N'-methylene bisacrylamide (MBAAm, Sigma-Aldrich), ammonium persulfate (APS, J&K Scientific), N,N,N',N'-n-tetramethylethylenediamine (TEMED, J&K Scientific), calcium chloride (CaCl₂, Sigma-Aldrich), sodium alginate (SA, Sigma-Aldrich), Rhodamine B (RhB, Sigma-Aldrich), methyl blue (methyl blue, Sinopharm), methylene blue (methylene blue, Sinopharm), Methyl violet (Methyl violet, Sinopharm), Methyl orange (Sinopharm), methyl green (Sinopharm), polytetrafluoroethylene membrane (PTFE), AAO template (Whatman), PVDF base membrane. All materials used in the experiment were not treated before use.

2.2 Preparation of polyacrylamide hydrogel

Polyacrylamide hydrogels are prepared by common free radical polymerization. The specific proportion of each material is as follows: deionized water: acrylamide monomer: N,N'-methylene bisacrylamide: ammonium persulfate = 100: 15: 0.3: 0.3, configured into a uniform aqueous solution and add 1 wt% tetraethylenediamine, quickly stirred and evenly cast into the template to obtain a polyacrylamide hydrogel with a specific shape, then immersed the prepared polyacrylamide hydrogel in deionized water to make it fully swell and remove the unreacted monomers in the free radical polymerization reaction. Immerse the fully swollen polyacrylamide hydrogel in calcium chloride aqueous solution for 24 h for standby.

2.3 Preparation of calcium alginate filtration membrane

The preparation method of pure calcium alginate filtration membrane is shown in Figure 2. The polyacrylamide hydrogel that soaked completely in the calcium chloride solution is placed under silicone oil to form an oil/ gel interface. The sodium alginate prepolymer is configured, and the independently built test bench is used to automatically realize the movement of the liquid, so that the polymer liquid (a small amount of RhB solution is added for observation, it has no effect on the solution spreading) can achieve super spreading to form a liquid film at the gel interface, and can be fully cross-linked with calcium chloride in gel to form calcium alginate gel film. After fully crosslinking for 5min, transfer the gel film to a water tank filled with deionized water. At this time, the calcium alginate gel film polymerized on the gel surface is peeled off from the hydrogel substrate to remove the excess silicone oil, washed with ethanol, then transferred to different porous filtration membrane substrates, and dried in an oven to obtain dry pure calcium alginate filtration membranes.

2.4 Characterization

Field emission scanning electron microscope (SEM, JEOL JSM8010) to observe the surface morphology and cross-section of the sample, ultraviolet spectrophotometer (UV-vis, SHIMADZY Japan).

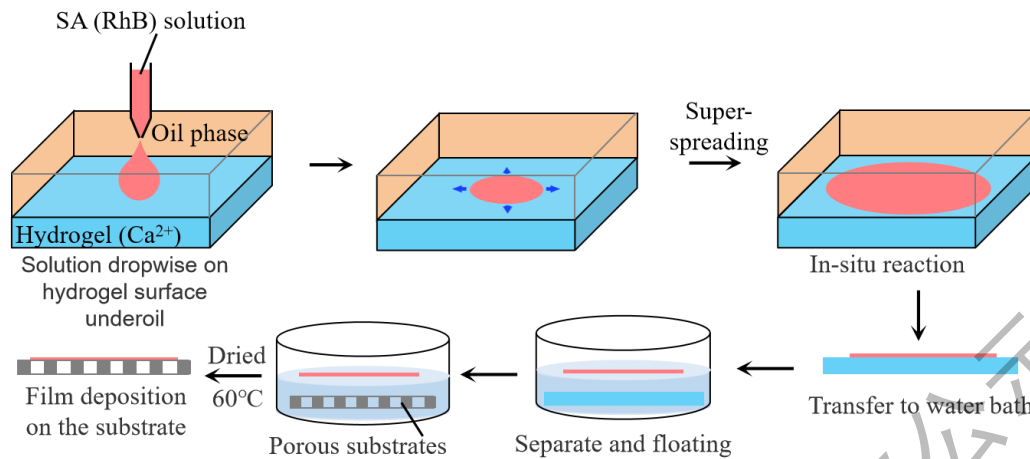


Figure 2. Schematic of the preparation process for calcium alginate filtration membranes via superspreading process on hydrogel surfaces under silicon oil and transfer to a porous support poly(vinylidene fluoride (PVDF) or anodised alumina). Concentrations of alginate in water used for dropping were in the range from 0.13 to 0.4 wt%. (Small amount of red dye Rhodamine B (0.02 g/L) is used here for clear observation, but it would not influence the spreading of the reaction solution).

3. Results and Discussion

3.1 Characterization of calcium alginate filtration membrane

Figure 3 shows an optical photograph and micromorphology of the calcium alginate filtration membrane. Figure 3a is an optical photo of CA filtration membrane on the PVDF support substrate. It can be seen from the photo that the filtration membrane emits colorful colors similar to the shell surface under the sun. The transparency is high, which is mainly caused by its thin thickness. Figure 3b is a photo of the support substrate PVDF. It can be seen from the figure that the pore size of the PVDF substrate is about 200 nm. The pore channels are distributed in a network. The large pore size support substrate can not only improve the mechanical properties as a substrate, but

also serve as an ultrafiltration membrane for preliminary filtration; Figure 3c is an optical photo of the calcium alginate filtration membrane transferred to the AAO template. Because the surface of AAO is smooth, the reflection effect is stronger than that of PVDF, so the color is more obvious. Figure 3d is a scanned image of the AAO support substrate. The pore size of the AAO template is about 220 nm. Because the transmission channel of the AAO template is straight up and down, the filtration rate will be better than that of PVDF with network structure, but the mechanical performance of the AAO template is relatively poor, attention should be paid to the storage of the transfer film.

Figure 4 is a scanning image of the upper surface and interface of calcium alginate thin films prepared at different concentrations of sodium alginate. The mass fraction of sodium alginate in a-d is 0.13wt%, 0.17 wt%, 0.24 wt% and 0.4 wt%, respectively. The specific solution components are shown in Table 1.

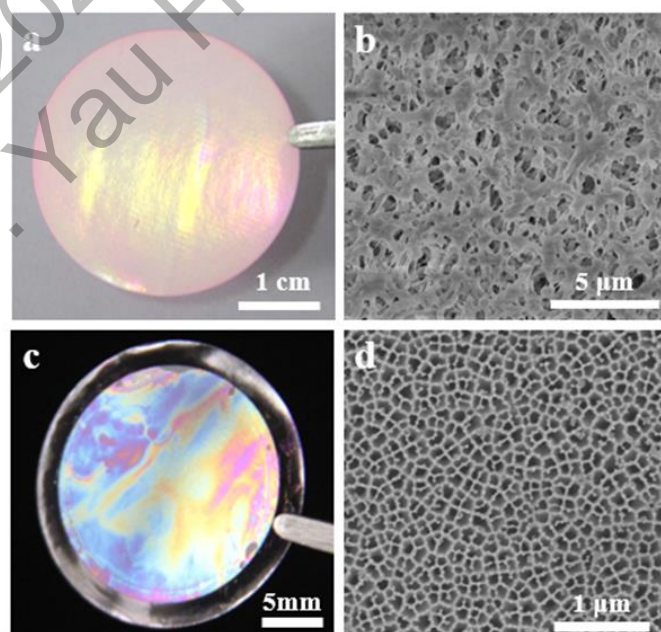


Figure 3 Optical and microscopic images of the prepared CA membranes. a) Digital photo of a CA membrane covering on a PVDF support with diameter of ≈ 25 mm. b) Top-view SEM image of the PVDF support with pores ≈ 200 nm. c) Digital photo of a CA membrane covering on a AAO support with diameter of ≈ 25 mm. d) Top-view SEM image of the AAO support with pores ≈ 220 nm.

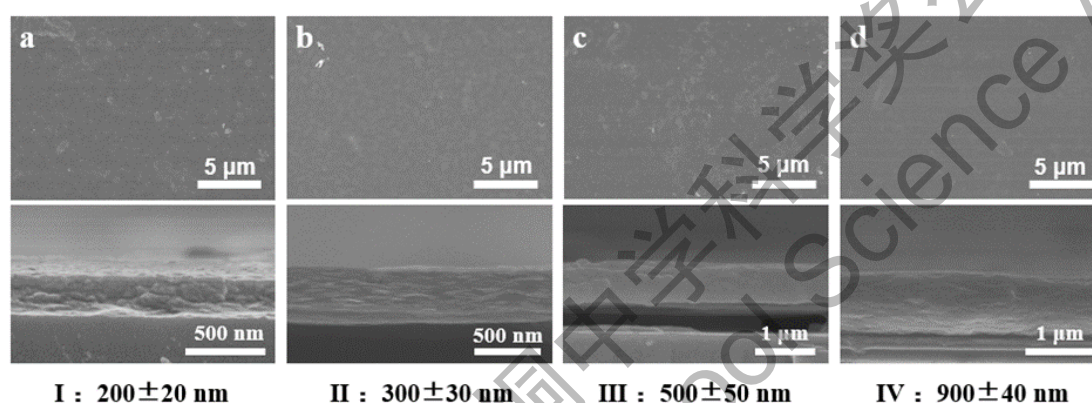


Figure 4. SEM image of calcium alginate thin films prepared at different concentrations of sodium alginate. The mass fraction of sodium alginate is a) 0.13 wt%, b) 0.17 wt%, c) 0.24 wt% and d) 0.4 wt%

By observing the upper surface scanning image, it can be found that with the increase of sodium alginate concentration, the surface morphology of calcium alginate film is relatively stable, no bulge or fold structure; It can also be found from the cross-sectional image that the thickness of the CA filtration membrane gradually increases with the increase of the concentration of sodium alginate. This is mainly because when the concentration of SA increases, the number of free polymer chains increases, the reaction is intense when combined with Ca^{2+} . Therefore, when the prepolymer liquid contacts and reacts with CaCl_2 in the gel substrate, a polymer film is grown at the gel

interface. With the progress of the reaction and the increase of SA concentration, more and more SA participated in the reaction, the polymer film was gradually improved and the film thickness increased.

Table 1. Composition of calcium alginate film prepolymer with different concentrations

	I	II	III	IV
SA(2 wt%)/ μl	300	300	300	300
H ₂ O/ μl	4000	3000	2000	1000
RhB/ μl	100	100	100	100

3.2 Selection of filter dye and determination of standard equation

According to the different charge types of organic dyes, they can be divided into the following categories: electrically neutral: rhodamine B; Cationic dyes: methyl green, methylene blue and methyl violet; anionic dyes: methyl orange and methyl blue. Various kinds of organic dyes with different concentrations were configured respectively, and the UV absorption peak was measured by UV spectrophotometer, as shown in Figure 5.

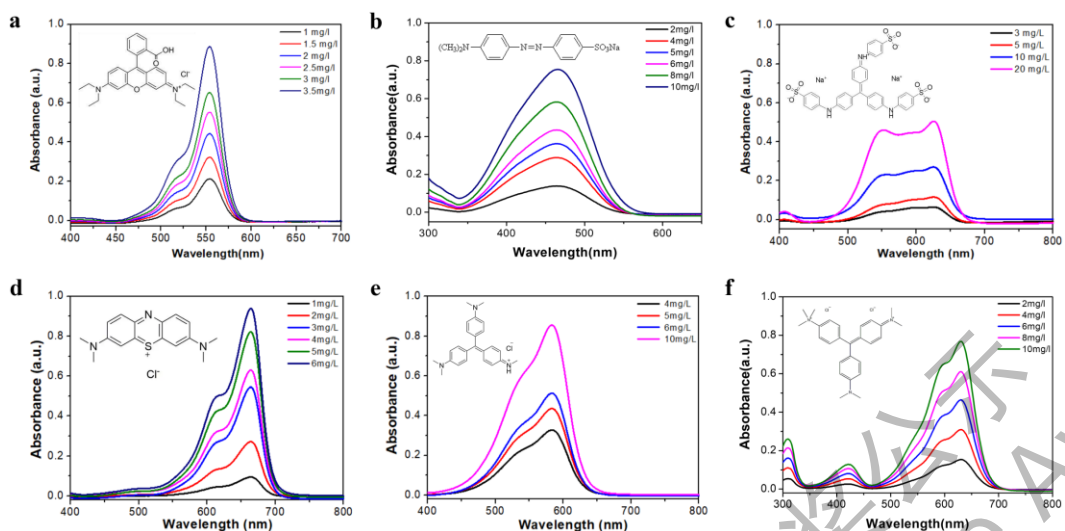


Figure 5. UV visible absorption spectra of different dyes a) Rhodamine B; b) Methyl orange; c) Methyl blue; d) Methylene blue; e) Methyl violet; f) Methyl green

Through the origin curve, data fitting is carried out, and the specific fitting equations are as follows (3.1) - (3.6) (X is the dye concentration (mg/L), Y is the absorption peak intensity (a.u.):

$$\text{Rhodamine B (neutral): } Y=0.22366X-0.0107 \quad (3.1)$$

$$\text{Methyl orange (negative): } Y=0.0762X-0.018 \quad (3.2)$$

$$\text{Methyl blue (negative): } Y=0.02601X-0.00833 \quad (3.3)$$

$$\text{Methylene blue (positive): } Y=0.17049X-0.04687 \quad (3.4)$$

$$\text{Methyl violet (positive): } Y=0.08669X-0.00854 \quad (3.5)$$

$$\text{Methyl green (positive): } Y=0.0765X+0.0022 \quad (3.6)$$

According to the fitting equation, the relationship between the absorption peak strength and different dye concentrations can be understood, which is of great significance for the calculation of later filtration performance. All the above dyes are configured into a certain concentration of dye solution, and the filtration experiment is carried out at room temperature.

3.3 Effect of membrane thickness on filtration performance

Generally, there are two main factors affecting membrane flux: Film thickness and film structure. If the thickness of the filtration membrane is large, the particle transport distance is increased and the membrane flux will be reduced, the filtration performance of the filtration membrane will be affected. Therefore, the thinner the membrane is, the more favorable the flux is: at the same time, the surface structure, holes and wrinkles of the membrane will also play a role in promoting the increase of the membrane flux. Adjusting the volume fraction of sodium alginate in the solution can effectively change the mass fraction of sodium alginate in the polymer solution. As has been discussed above, changing the concentration of sodium alginate will also change the overall thickness of calcium alginate filtration membrane. When the concentration of SA changes from 0.13 wt% to 0.4 wt%, the thickness increases from 200 nm to 900 nm. The specific thickness change trend is shown in Figure 6.

When the thickness of CA filtration membrane increases from 200 nm to 800 nm, the flux to 4 mg/L rhodamine B solution shows a downward trend, while the rejection rate is relatively stable, as shown in Figure 6b. The main reason is that the increase of the thickness hinders the transport of dye molecules, only allowing water molecules to pass through. At the same time, with the increase of the film thickness, the density of the internal network is high, and the rejection effect on dye molecules is increased. When the thickness of the filtration membrane reaches a value, the rejection of dye by the filtration membrane is stable, with the increase of calcium alginate film thickness, the rejection rate is relatively stable, which indicates that the film thickness no longer

affects the rejection rate of the film and reaches a stable state; The decrease of flux indicates that the film thickness increases, which hinders the transport of substances. In Figure 6b, F refers to 4mg/L RHB solution, and P refers to the filtrate after filtration. It can be seen that the color decreases and the filtration effect is very obvious. At this time, the rejection rate can reach 97%.

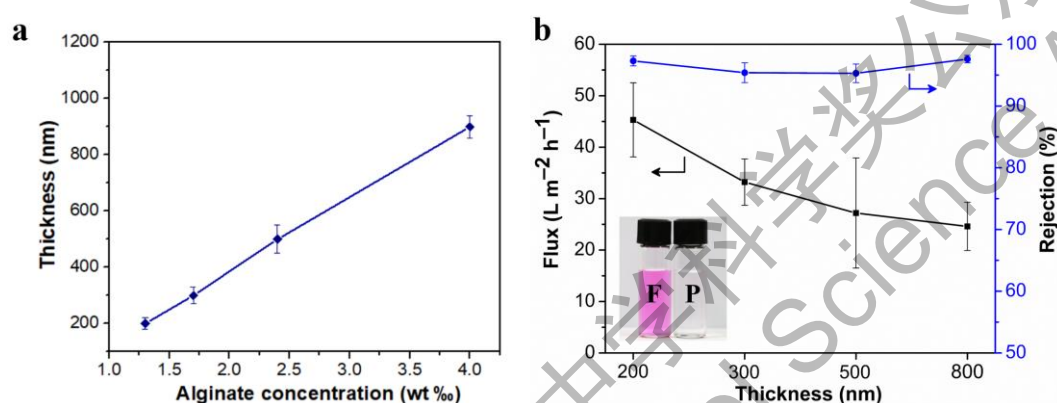


Figure 6. Thickness and filtration performance of CA membrane a) The variation trend of CA film thickness with SA concentration; b) Filtration performance of different thickness filtration membranes on RhB (RhB concentration is 4 mg/L)

3.4 Filtration property of CA membrane for different dye molecules

Because the thickness of the membrane will affect the filtration performance of CA, a 200 nm thick filter membrane was prepared and used in the filtration experiments of different dyes. Previous studies have shown that methyl green, methylene blue and methyl violet solutions are positively charged, methyl orange and methyl blue are negatively charged, while rhodamine B is neutral. When the filter membrane intercepts particles, in addition to the size effect of the pore size, there is also the charge interaction between them. Therefore, the rejection effect of the filtration membrane on dyes with different charges is also different.

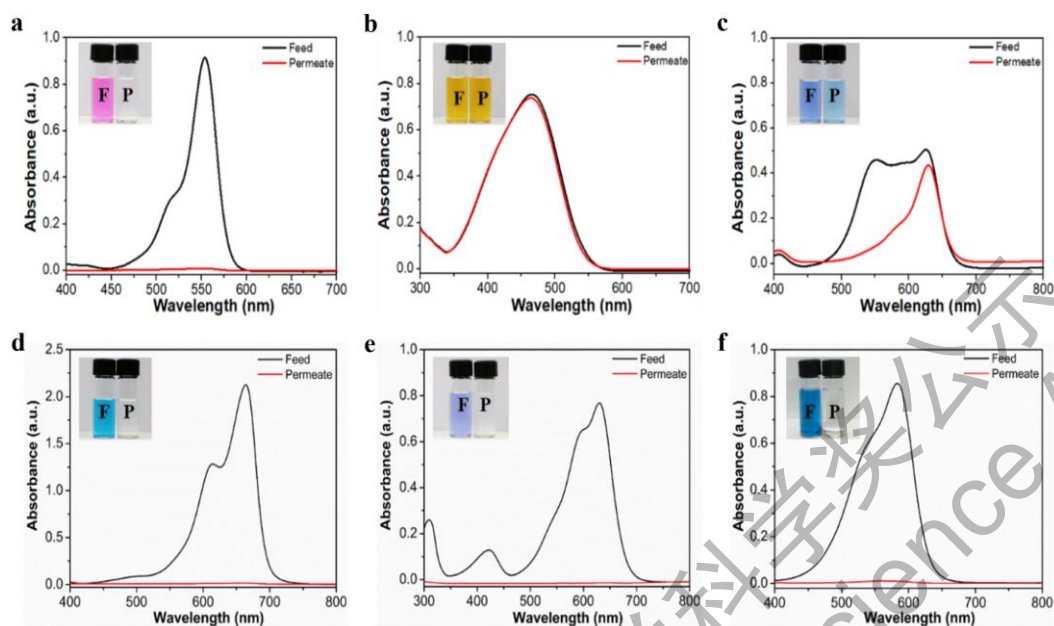


Figure 7. Filtration performance of calcium alginate membrane a) Rhodamine B (4 mg/L); b) Methyl orange (10 mg/L); Methyl blue (20 mg/L); d) Methylene blue (10 mg/L); e) Methyl violet (10 mg/L); f) Methyl green (10 mg/L)

Six dyes with different charges are used in the filtration experiment, the pressure is 0.2 MPa. After the water output is stable, the water output is weighed in unit time and the ultraviolet absorption of the filtrate is detected. The waiting time is more than 30 minutes. It can be found from Figure 7 that the calcium alginate membrane has a good rejection performance for electrically neutral and positively charged dyes, while the rejection performance for negatively charged dyes is almost zero. The main reason is that the calcium alginate nanofiltration membrane is also negatively charged. Due to the principle of "homogeneity attracts and anisotropy repels", the CA membrane has an excellent electrostatic absorption effect for electrically neutral and positively charged dye molecules. It can intercept most of the dye molecules and prevent them from

passing through the filter membrane; For the dye molecules with negative charges in solution, due to electrostatic repulsion, the dye molecules are difficult to adsorb on the surface of the filter membrane, so most of the dye molecules can pass through the filter membrane, and the rejection rate is low. Rhodamine B solution is a neutral solution, and calcium alginate membrane has an excellent rejection effect. Figure 8 shows the change of adhesion on the surface of calcium alginate gel membrane before and after filtration, indicating that the rejection effect of calcium alginate membrane on Rhodamine B is very obvious.

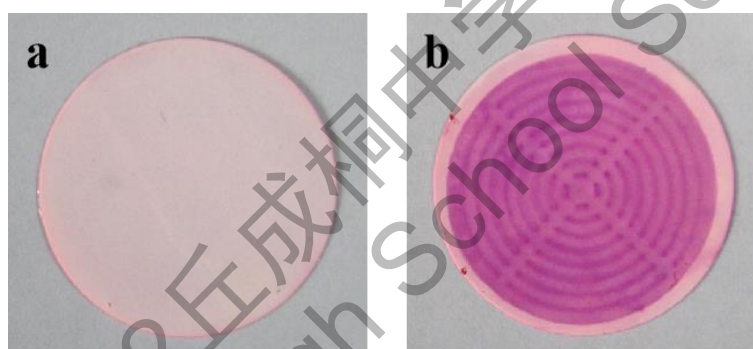


Figure 8. Comparison before and after calcium alginate filtration membrane. Filtration experiment of CA membrane on 4mg/L RhB solution a) before filtration: b) after filtration

Table 2. Filtration test results of different dyes by calcium alginate membrane

Solution	Thickness 200 nm				
	Mw (g mol ⁻¹)	Charge	Concentration (mg/L)	Permeance (L m ⁻² h ⁻¹ bar ⁻¹)	Rejection (%)
Rhodamine B	479.01	Neutral	4	45.3±7.2	97.3±0.8

Methyl green	458.47	+	10	66.3±6.4	99.8±0.1
Methylene blue	319.85	+	10	31.9±6.6	94.2±2.1
Methyl violet	408.03	+	10	29.1±3.5	97.2±0.5
Methyl orange	327.33	-	10	30.5±6.5	0.9186±0.3
Methyl blue	799.8	-	20	42.8±10.3	7.02±5

The experimental results further prove the filtration results of calcium alginate membrane for different charged dyes. Because methyl green, methylene blue and methyl violet dyes are positively charged, the filtration effect of calcium alginate gel membrane is very obvious, of which the filtration effect of methyl green can reach 99.8%, and the relatively poor one of methylene blue is 94.2%; Rhodamine B dye is neutral and has a very good rejection efficiency of 97.3%. Methyl orange and methyl blue dyes are negatively charged, and the rejection rate of calcium alginate film is less than 10%. It is worth noting that the molecular weight of methyl blue reached 800, the rejection rate is still very low, which indicates that the filtration experiment of calcium alginate membrane for different organic dyes mainly depends on the charge of different dyes rather than on the size of particles.

4. Conclusion

In this experiment, we have utilized the superspreading of SA solution on the immersed hydrogel surfaces to produce large-area, uniform thin CA membranes supported on various porous substrates. The completely spreading of dilute solution and

the rapid in situ Ca^{2+} -induced crosslinking of SA resulting the CA membranes with the nanoscale thickness. Therefore, the prepared CA membranes exhibit high retention (> 94%) for positively charged and neutral organic molecules. More importantly, because of the scalable production, this method can broaden the practical application of high-performance CA membranes or CA-based nanocomposites.

仅用于2022丘成桐中学科学奖公示
2022 S.-T. Yau High School Science Awards

5. Acknowledgement

The author would like to thank Professor Mingjie Liu and his research team for their help in the experiment. Under the guidance of Professor Liu and the help of Dr. Chuangqi Zhao, the author Liu Yunhao independently completed all the experiments in this thesis. I hereby sincerely thank all of the people who contributed to this research project and paper

仅用于2022丘成桐中学科学奖公示
2022 S.-T. Yau High School Science Awards

6. References

- [1] Carneiro P. A., Umbuzeiro G. A., Oliveira D. P., et al. Assessment of water contamination caused by a mutagenic textile effluent/dyehouse effluent bearing disperse dyes[J]. *Journal of Hazardous Materials*, 2010, 174: 694-699.
- [2] He Y., Li G., Wang H., et al. Effect of operating conditions on separation performance of reactive dye solution with membrane process[J]. *Journal of Membrane Science*, 2008, 321: 183-189.
- [3] Giri A., Goswami N., Pal M., et al. Rational surface modification of Mn₃O₄ nanoparticles to induce multiple photoluminescence and room temperature ferromagnetism[J]. *Journal of Materials Chemistry C*, 2013, 1: 1885-1895.
- [4] Zhang R., Zhou T., Peng H., et al. Nanostructured switchable pH-responsive membranes prepared via spherical polyelectrolyte brushes[J]. *Journal of Membrane Science*, 2019, 580:117-124.
- [5] Kappel C., Kemperman A. J., Temmink H., et al. Impacts of NF concentrate recirculation on membrane performance in an integrated MBR and NF membrane process for wastewater treatment[J]. *Journal of Membrane Science*, 2014, 453: 359-368.
- [6] Ma H., Burger C., Hsiao B. S., et al. Highly Permeable Polymer Membranes Containing Directed Channels for Water Purification[J]. *ACS Macro Letters*, 2012, 1: 723-726.
- [7] La Y., McCloskey B., Sooriyakumaran R., et al. Bifunctional hydrogel coatings for water purification membranes: Improved fouling resistance and antimicrobial activity [J]. *Journal of Membrane Science*, 2011, 372: 285-291.
- [8] Kang G., Cao Y., Zhao H., et al. Preparation and characterization of crosslinked poly(ethylene glycol) diacrylate membranes with excellent antifouling and solvent-resistant properties[J]. *Journal of Membrane Science*, 2008, 318: 227-232.
- [9] Xie L., Hong F., He C., et al. Coatings with a self-generating hydrogel surface for antifouling[J]. *Polymer*, 2011, 52: 3738-3744.

- [10] Lei J., Ulbricht M. Macroinitiator Mediated Photoreactive Coating of Membrane Surfaces with Antifouling Hydrogel Layers[J]. *Procedia Engineering*, 2014, 455: 207-218.
- [11] Zhang W., Xu Y., Yu Z., et al. Separation of acetic acid/water mixtures by pervaporation with composite membranes of sodium alginate active layer and microporous polypropylene substrate[J]. *Journal of Membrane Science*, 2014, 451: 135-147.
- [12] Suratago T., Taokaew S., Kanjanamosit N., et al. Development of bacterial cellulose/alginate nanocomposite membrane for separation of ethanol–water mixtures[J]. *Journal of Industrial and Engineering Chemistry*, 2015, 32: 305-312.
- [13] Feng L., Cao Y., Xu D., et al. Molecular weight distribution, rheological property and structural changes of sodium alginate induced by ultrasound[J]. *Ultrasonics Sonochemistry*, 2017, 34: 609-615.
- [14] Li Y., Jia H., Cheng Q., et al. Sodium alginate–gelatin polyelectrolyte complex membranes with both high water vapor permeance and high permselectivity[J]. *Journal of Membrane Science*, 2011, 375(1-2): 304-312.
- [15] Mahmood A., Bano S., Kim S. G., et al. Water–methanol separation characteristics of annealed SA/PVA complex membranes[J]. *Journal of Membrane Science*, 2012, 415-416(1): 360-367.
- [16] Yang J. M., Wang N. C., Chiu H. C. Preparation and characterization of poly(vinyl alcohol)/sodium alginate blended membrane for alkaline solid polymer electrolytes membrane[J]. *Journal of Membrane Science*, 2014, 457: 139-148.
- [17] Ji C. H., Xue S. M., Xu Z. L. Novel Swelling-Resistant Sodium Alginate Membrane Branching Modified by Glycogen for Highly Aqueous Ethanol Solution Pervaporation[J]. *ACS Applied Materials & Interfaces*, 2016, 8(40): 27243-27253.
- [18] Moulik S., Nazia S., Vani B., et al. Pervaporation separation of acetic acid/water mixtures through sodium alginate/polyaniline polyion complex membrane. *Separation and Purification Technology*, 2016, 170: 30-39.

- [19] Yang J. M., Yang J. H., Tsou S. C., et al. Cell proliferation on PVA/sodium alginate and PVA/poly(γ -glutamic acid) electrospun fiber[J]. Materials Science and Engineering: C, 2016, 66: 170-177.
- [20] Rana D., Matsuura T. Surface modifications for antifouling membranes[J]. Chemical reviews, 2010, 110(4): 2448-2471.
- [21] La Y. H., Sooriyakumaran R., McCloskey B. D., et al. Enhancing water permeability of fouling-resistant POSS-PEGM hydrogels using ‘addition-extraction’ of sacrificial additives[J]. Journal of Membrane Science, 2012, 401-402: 306-312.

2022 S.-T. Yau High School Science Awards
仅用于2022丘成桐中学科学奖公示